Digest Journal of Nanomaterials and Biostructures Vol. 14, No. 3, July - September 2019, p. 683 - 693

PALLADIUM/ SILICON OXIDE/ SILICON CARBIDE NANO-STRUCTURES FOR SENSITIVE DETECTION OF HYDROGEN

A. S. NEAMȚU[a], D. OVEZEA[b], J. NEAMȚU[b,*]
[1]*National Institute for Aerospace Research "Elie Carafoli", Bd. Iuliu Maniu No. 220, Bucharest, Romania*
[2]*National Institute for Research & Development in Electrical Engineering, Splaiul Unirii No. 313, Bucharest, 030138, Romania*

This paper is an investigation of palladium/silicon oxide/4H-SiC nanostructures with applicability for sensitive detection of hydrogen in severe conditions such as: high temperature and corrosive environments. The palladium/silicon oxide/4H-SiC nanostructures were fabricated using microelectronics technology. Silicon carbide (4H-SiC) semiconductor is the substrate for Metal/Oxide/Semiconductor (MOS) nanostructure. The insulator quality represents an important factor for the MOS micro-sensor. A thin film of palladium acts as a catalyst for the dissociation of hydrogen molecules. The electrical characteristics of MOS nanostructure in presence of hydrogen gas are well connected with low concentrations of hydrogen. Pd/SiO_2/SiC can be used for hydrogen leakages detection.

(Received April 11, 2019; Accepted August 16, 2019)

Keywords: Silicon carbide, Thin films, Hydrogen sensor, MOS structure, Palladium

1. Introduction

Electronic sensors are important in various applications for safety reasons [1–4]. They are of great importance mainly for detection of hydrogen leakage [2,5], below the lower explosive limit of 4% by volume ratio of hydrogen to air [3]. Hydrogen gas is a major cause of corrosion of hydrogen tanks in chemical and aerospace industries [6]. Hydrogen atoms that are' absorbed as low as 1ppm can cause cracking [7] and damages of space and aerospace engines. This problem is very actual after serious accidents involving hydrogen, such as the tragedy of the destruction of Space Shuttle Challenger and the death of her crew due to fuel leakage. Hence, in order to avoid the leakage of hydrogen which can cause serious explosions, sensors that can detect hydrogen quickly and accurately are essential in practical applications [8]. These hydrogen sensors are required to operate at high temperatures and under potentially corrosive conditions [8, 9].

Although semiconductor devices such as Metal/Oxide/Semiconductor (MOS) capacitors, Schottky diodes and field effect transistors were developed first time on silicon (Si) substrates for gas sensors [10], when it comes to operation at temperatures above 150°C, the electrical properties of silicon are strongly degraded, because of self-heating at high power levels. Besides, pure Si sensors containing *pn* junctions for electrical isolation exhibit a serious drawback which is the main cause that they cannot be used at temperatures above 150◦C. It is important to state that superior properties in the field of high temperature and high power applications can be estimated by comparing band gap and breakdown voltage of the semiconductors [11]. Thus, most electronic devices, hydrogen sensors in this case, which simultaneously require high temperature and high power operation, will necessarily be realized using wide bandgap devices. Presently, silicon carbide (SiC) appears to be the strongest candidate wide bandgap semiconductor for harsh environment applications [12]. Single-crystal SiC wafers have been commercially available for nearly two decades. Silicon carbide offers advantages in some important areas of technology, such as better control of crystal impurities needed to realize electronic devices. SiC crystals have crystal

* Corresponding author: jenica.neamtu@gmail.com

dislocation defects fewer than other wide bandgap semiconductors. It also has excellent mechanical properties, specifically, hardness and wear resistance [13]. In terms of hardness, SiC has a Mohs hardness of 9, which compares favorably with values for other hard materials such as diamond (10) and topaz (8). In terms of wear resistance, SiC has a value of 9.15, as compared with 10.00 for diamond. SiC has a high thermal conductivity (better than Cu), and for some polytypes (notably 4H and 6H), has a high critical electric field (in excess of $2MVcm^{-1}$), which is one order of magnitude higher than of Si.

In this context, thin films nanostructures based on silicon carbide (SiC) semiconductor become valuable hydrogen gas sensors. Most of the SiC-based H_2 sensors are grouped into field effect devices, with properties determined largely by the effect of an electric field on a region within the devices. The unique working principle of SiC field effect devices gives gas sensors, based on them, high sensitivity and good selectivity and reliability towards H_2 gas sensing [14]. Among these field effect devices, metal-oxide-semiconductor (MOS) capacitor is preferred as H_2 sensor.

The MOS capacitor consists of a thin oxide layer sandwiched between a metal layer and a semiconductor substrate, which act as electrodes [15]. The film of metal acts as catalyst for gas molecules adsorption and this role governs selection of both metal type and deposition technology. It can be a very thin film, with a high surface area, but also it can be porous, thicker and stable at high temperatures. The choice of the catalytic metal depends on the type of gas which has to be detected. For hydrogen detection, metals such as Pt, Pd and Ni are most suitable [14-16]. The MOS capacitors require a dielectric oxide for the modulation of the semiconductor carrier concentration via an applied gate potential [9]. This thin film of dielectric oxide deposited on SiC semiconductor can be silicon oxide (SiO_2) [15], titanium oxide (TiO_x) [16], zinc oxide (ZnO) [17] or tungsten oxide (WO_3) [18].

The electric operation of MOS structure as micro-sensor is dominated by electronic interactions at the interfaces. These interfaces are the ambient gas /metal interface, the metal/oxide interface and the oxide/semiconductor interface [19, 20].

The goal of this paper is the study the palladium/silicon oxide/4H-SiC nanostructures used as hydrogen micro-sensor. All thin films of palladium and silicon oxide were fabricated by high vacuum sputtering depositions. The semiconductor used as substrate was 4H-SiC wafer, with two epitaxial layers: a layer with thickness of 0.5 μm and an active doped layer ($N_D=2.07x10^{16}$ cm^{-3}) with a thickness of 8 μm. The main electrical characteristics of $Pd/SiO_2/SiC$ structures in correlation with hydrogen concentrations are discussed. The flat band voltage has an important decrease when H_2 concentration rises and reaches a -4.05 V shift at the highest studied concentration, 2000 ppm H_2. The saturation tendency of the sensor at higher concentration of H_2 for high temperatures (over 150°C) is due to the action of hydrogen that is partially eliminated at the metal/oxide interface.

2. Sensing mechanism towards hydrogen by metal/oxide/silicon carbide thin film structure

The mechanism enabling hydrogen sensitivity of devices based on silicon or silicon carbide semiconductors was described by Lundström et al. [10, 21, 22]. When the surface of metallic thin film of MOS capacitor is exposed to hydrogen gas, the molecules dissociate at the surface of the metallic thin film and convert in hydrogen atoms. Some of the hydrogen atoms remain at the surface of the metal, and others diffuse into the metal until they reach the metal-oxide interface. There is equilibrium between the number of hydrogen atoms adsorbed at the metal surface and the number of atoms adsorbed at the metal-oxide interface. The hydrogen atoms from the metal-oxide interface are polarized and create a bipolar layer. This bipolar layer decreases the semiconductor work function, which reduces the flat band voltage of the MOS capacitor. The change of the flat band voltage determines a shift of the C-V characteristics of the capacitor [23, 24]. Fig. 1 shows the mobile charges and trapped charges to the oxide and oxide-semiconductor interface.

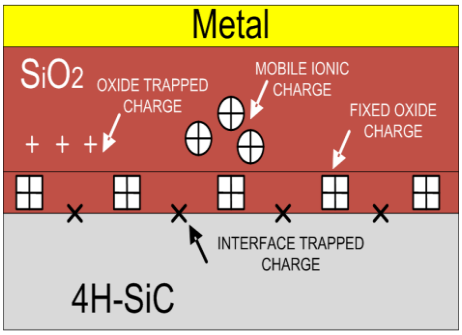

Fig. 1. The charges in oxide and on the interfaces of the MOS structure

The oxide charges include four types of charges: trapped charges at oxide-semiconductor interface, fixed oxide charges, trapped oxide charges and mobile ionic charges.

The last three types of charges, distributed inside the oxide, are positive and create a depletion region at the surface of the 4H-SiC semiconductor layer. This region modifies the flat band voltage of the MOS capacitor. An adjustment of the electrical charge in the depletion region of the semiconductor occurs for any voltage applied on the thin film metal [25].

The response towards hydrogen of a MOS capacitor has been derived from the Langmuir adsorption isotherm equations, which relates to the voltage shift (ΔV) induced in the *C-V* characteristics of the gas concentration [10, 22].

At the surface of the metallic thin film takes place a dissociation of hydrogen molecules:

$$H_2 \leftrightarrow 2H \tag{1}$$

The kinetic equations for the transport of hydrogen in the metallic thin film at equilibrium state are:

$$\frac{n_i}{N_i - n_i} = k_s \frac{n_s}{N_s - n_s}, and$$
$$\frac{n_s}{N_s - n_s} = \left[\frac{c_1}{d_1} P(H_2) \right]^{1/2} \tag{2}$$

where N_s and N_i are the number of adsorption sites at the metal surface and metal-oxide interface respectively, n_s and n_i are the number of hydrogen atoms adsorbed at the metal surface and metal-oxide interface respectively. k_s and K are constants that depend on the difference between the adsorption energy at the metal surface and the adsorption energy at the interface, c_1 and d_1 are constants of forward and backward reaction rate at the metal surface, and $P(H_2)$ is the hydrogen partial pressure.

The coverage of hydrogen at the metal surface (θ_s) and at the interface (θ_i) are:

$$\theta_s = \frac{n_s}{N_s}, \text{ and } \theta_i = \frac{n_i}{N_i} \tag{3}$$

The coverage of hydrogen at the metal-oxide interface can be expressed as a function of the hydrogen partial pressure:

$$\theta_i = \frac{K\left[P\left(H_2\right)\right]^{1/2}}{1+K\left[P\left(H_2\right)\right]^{1/2}} \tag{4}$$

The output signal of the MOS capacitor is the voltage shift (ΔV) induced in the *C-V* characteristic. The connection between θ_i and the voltage shift (ΔV) is obtained by assuming that the shift (ΔV) is proportional to the coverage of hydrogen atoms at the interfaces.

$$\Delta V = \Delta V_{\max}\theta_i \tag{5}$$

where ΔV_{max} is the maximum shift of the *C-V* characteristic when the adsorption sites at the interface are fully saturated ($\theta_i = 1$). Finally, from Equations (4) and (5) the voltage change in *C-V* characteristic can be expressed also as a function of the hydrogen partial pressure:

$$\Delta V = \Delta V_{\max}\frac{K\left[P\left(H_2\right)\right]^{1/2}}{1+K\left[P\left(H_2\right)\right]^{1/2}} \tag{6}$$

3. Experimental

The ($Pd/SiO_2/SiC$) structures were fabricated on n-type 4H-SiC wafers, 0.015-0.028 x 10^{-2} ohm·m resistivity, with two epitaxial layers: a buffer layer with thickness of 0.5 μm and the doped (N_D=2.07x10^{16} cm^{-3}) active layer with a thickness of 8 μm.

Prior the sputtering depositions the 4H-SiC wafer was cleaned in two RCA solutions. For the organic contaminants elimination, the solution was composed of ammonia, hydrogen peroxide and deionzed water. For the ionic elements elimination, the solution was composed of hydrochloric acid, hydrogen peroxide and deionized water.

The silicon oxide layer, with 50 nm thickness, was grown on the wafer by radio frequency (RF) sputtering, at 100 W incident power and the substrate temperature of 250^{o}C in 1x10^{-3} torr Ar (99.999%) atmosphere.

The electrode of palladium thin film, with 100 nm thickness, was obtained by direct current (DC) sputtering deposition, at 150 W in 5x10^{-3} torr Ar (99.999%) atmosphere. The circular dots with 300, 400 and 800 μm diameters were patterned using micro-lithography mask. The equipment used for thin film depositions was UHV Sputtering& E-Beam ATC-2200V, AJA International Inc.

Figure 2 shows a part of the mask with dots of 300, 400 and 800 μm diameter for the structures fabricated on n-type 4H-SiC wafers.

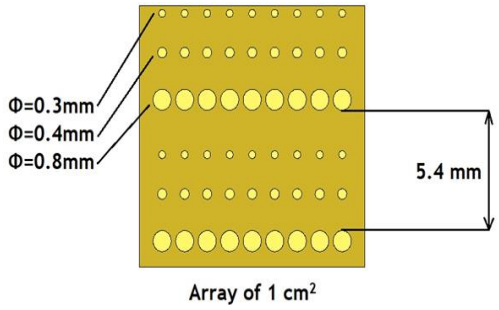

Fig. 2. Array of 1 cm^2 from mask with dots of 300, 400 and 800 μm diameters.

The ohmic contact on the back side of SiC substrate is an aluminum layer of 300 nm thickness, made by DC sputtering at $5x10^{-3}$ torr Ar (99.999%) atmosphere. The couple, the aluminum metallization and Al/Ni-Al bonding wires, shows good performance for all cases of devices used at high temperature [26].

The microstructures of Pd thin films were investigated by Field Emission Scanning Electron Microscopy using a (FE SEM-FIB) Zeiss-Auriga, Germany.

The homogeneity and the surface roughness of silicon oxide thin film and palladium thin films were analyzed with interferometric microscope Veeco NT1100.

Electrical characterization of $Pd/SiO_2/SiC$ nanostructures and electrical response at different H_2 concentrations (from 0 ppm to 2000 ppm) were investigated with an in-house developed gas sensor test equipment. Figure 3 shows a schematic of the measurement gas sensor equipment.

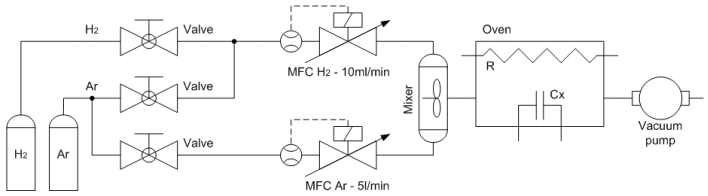

Fig. 3. Schematic of gas sensor measurement equipment.

Fig. 4 shows the fabricated gas sensor test equipment. The test equipment (fig. 4) is composed of: a gas mixing system with mass flow controllers (a), a sealed vacuum chamber and vacuum pump (b), sensor biasing adapter, signal conditioning system, heater, power supplies (c), digital LCR bridge (d).

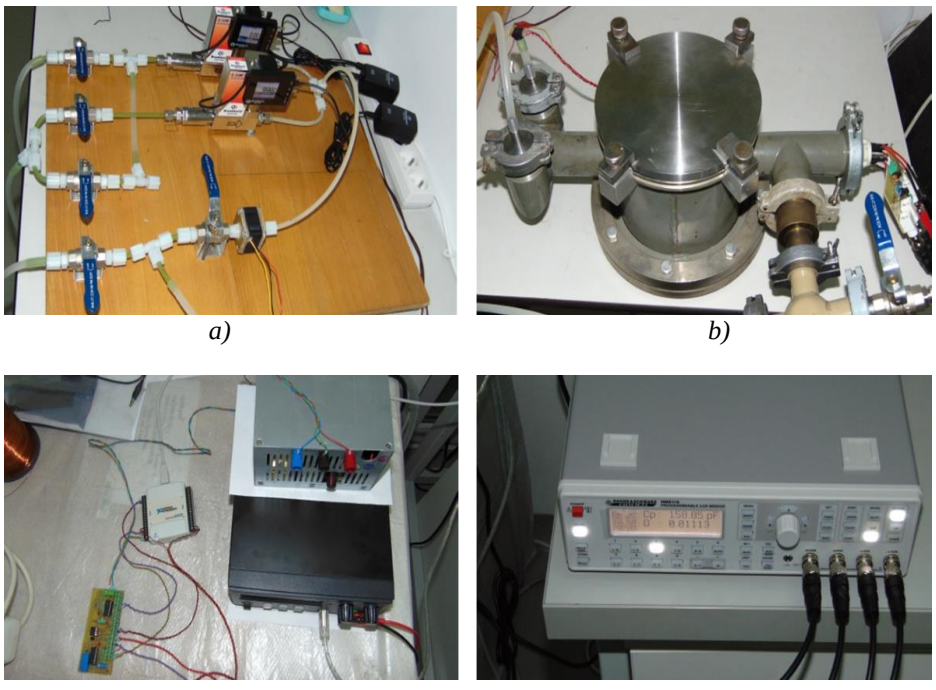

a) *b)*

c) *d)*

Fig. 4. Gas sensor test-equipment: a) gas mixing system, b) vacuum chamber, c) signal conditioner, d) HM8118 LCR bridge

The electrical test equipment has the following functions:

The gas mixing block is made of two mass flow controllers (MFC) and the gas mixer. By appropriate programming of the MFCs and using pressurized canisters of 0.5% and 5% H_2 :Ar, it is possible to achieve concentrations in the range of 0.3 ppm to 5000 ppm H_2.

The samples were heated with a special support mounted in the vacuum chamber. The support has two attached heating resistors for a total of 80 W of power, and a Pt100 sensor for temperature control. The temperature can be set between 50°C and 250°C, the maximum temperature being limited by the thermo-conductive adhesive used to attach the resistors. A pressure sensor was attached to the vacuum chamber for the purpose of monitoring the environment and checking the complete evacuation of the gases from the chamber.

The adapting circuit was necessary to generate the biasing voltage and for the conditioning of the signal received from the Pt 100 sensor. The temperature sensor was supplied by a constant current source type LM334Z with temperature drift compensation and a current of 1mA. The resulting voltage drop on the Pt100 was conditioned in order to have a 0-10V output for a temperature range of 30°C to 250°C. A calibration was done and the response curve was software compensated.

4. Results and discussion

4.1 Microstructure and surface roughness of Palladium thin film and SiO_2 thin film

The microstructures of the thin film of metal and the metal-oxide-SiC contacts are crucial to improve the electrical characteristics of the sensor [25]. It is desirable to obtain smooth and porous layers of palladium in order to increase the catalytic activity rate, which shall lead to improving the sensitivity of MOS structures [26]. Palladium thin film is very stable as catalyic metal at high temperature up to 700^{o}C [27].

Fig. 5 shows a detail of Pd/SiO_2/SiC structure. In it one can observe the porosity of palladium thin film.

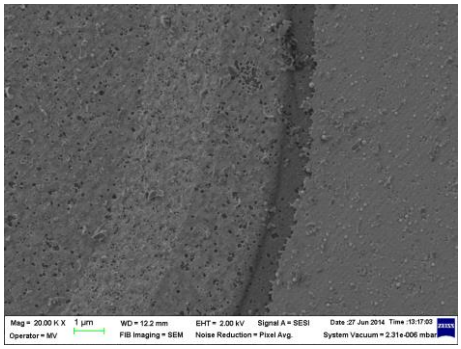

Fig. 5. Detail of Pd/SiO_2/SiC structure. Magnitude 20 000 x.

The porosity of palladium thin film facilitates the dissociation of hydrogen molecules and the diffusion of atoms from the metal thin film towards the metal-oxide and oxide-semiconductor interfaces.

Fig. 6 shows the microstructure of palladium thin film of 100 nm thickness, after DC sputtering deposition, investigated by Field Emission Scanning Electron Microscopy (FE SEM).

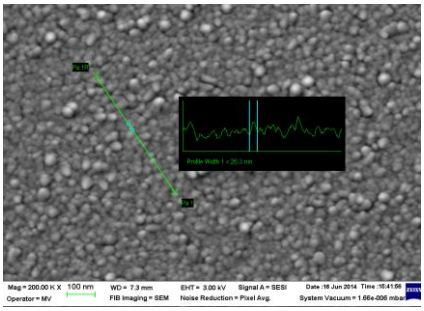

Fig. 6. Microstructure of Pd thin film (thickness of 100 nm), by Field Emission Scanning Electron Microscopy (FE SEM). Magnitude 200000 x.

The microstructure of as-deposited palladium thin film is very uniform and continuous. The qualitative medium grain size was between 20-30 nm.

Dimensional metrology for micro/nano-structure is crucial for understanding of the performance of micro-fabricated products. The Veeco NT1100 works in two modes. The PSI mode, based on optical phase-shifting, is dedicated to roughness measurements and VSI (Vertical Shift Interference) mode, is dedicated to topography and thickness measurements.

Fig. 7 shows the surface roughness: average roughness (Ra), quadratic roughness (Rq) and total roughness (Rt) of deposited Pd thin film gate.

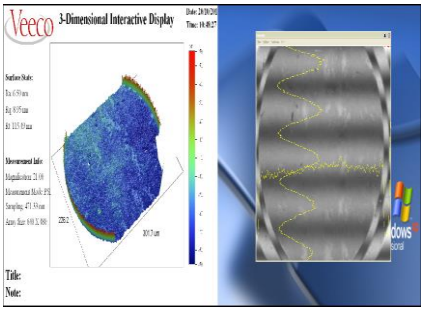

Fig. 7. The roughness analysis of Pd thin film surface.

The roughness of palladium thin film after DC sputtering deposition is: Ra=6.5 nm, R q=8.95 nm, R t=115.49 nm.

Fig. 8 shows the topography and thickness measurements of silicon oxide deposited by RF sputtering.

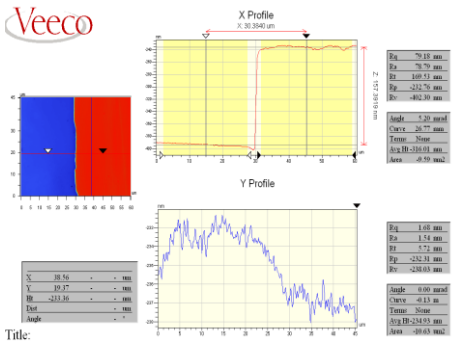

Fig. 8 The profile of silicon oxide thin film deposited by RF sputtering

The interlayer of silicon oxide increased by RF high vacuum sputtering is a good alternative to SiO_2 grown by thermal oxidation of SiC substrate. Often the growth of SiO_2 on silicon carbide semiconductor wafer leads to high levels of surface defects causing high interface charges to devices with poor channel mobility [25].

4.2 Electrical measurements of Pd/SiO_2/SiC nanostructures in the presence of hydrogen gas

Electrical measurements of MOS structures were carried out with the gas sensor measurement equipment described in Figs. 3 and 4. The MOS structures were measured in a vacuum chamber at temperatures between room temperature and 200^{o}C. Hydrogen comcentrations in the chamber were varied up to 2000 ppm. The samples were flushed with inert argon gas before exposure to hydrogen gas.

Fig. 9 shows the electrical response of Pd (100nm)/SiO_2 (50nm)/SiC nanostructures in the presence of hydrogen gas. The electrical characterization was made by measuring the capacitance versus bias voltage of the sensor, while exposed to various concentrations of hydrogen gas (from 0 ppm to 2000 ppm H_2: Ar). All measurements were made at a frequency of 100 kHz and an amplitude of 50 mV. The temperature was set at 150°C (lower than the maximum supported by the test stand) and the applied voltage was varied from -10V to 10V in 0.1V steps for each gas concentration.

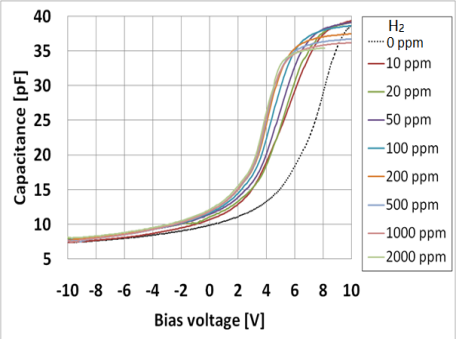

Fig. 9. Electrical response of MOS structure of H_2 concentrations from 0 ppm to 2000 ppm, measured to 150°C

It can be observed that an increase in hydrogen concentration creates a left displacement of the C-V curves towards negative voltages, as is discussed in [25, 26].

The minimum inversion capacitance is not affected by change in H_2 concentration, in accordance with the studies where a native oxide SiO_2 is used, i.e. [27].

Based on the response formula

$$R\%= (C_{H2} - C_{Ar})/ C_{Ar} *100[\%],$$

A bias voltage of 4.8V was found to achieve the best response for this nanostructure as hydrogen sensor. The data was extracted from figure 9. It can be observed that the sensor has a good response to hydrogen concentrations in the approximate range of 0-200 ppm, but easily saturates beyond.

The flat band voltage of real MOS structures is further affected by the presence of charge in the oxide or at the oxide-semiconductor interface. The flat band voltage corresponds to the voltage which is applied to the gate electrode and yields a flat energy band in the semiconductor. The flat-band voltage marks the beginning of the accumulation region in the C-V characteristic. Figure 10 presents the flat band voltage shift (ΔV) as a function of hydrogen gas concentration, measured to the temperature of 150°C. It was calculated from the measured capacitance [14] during bias voltage sweeps for hydrogen concentrations between 0 ppm-2000 ppm.

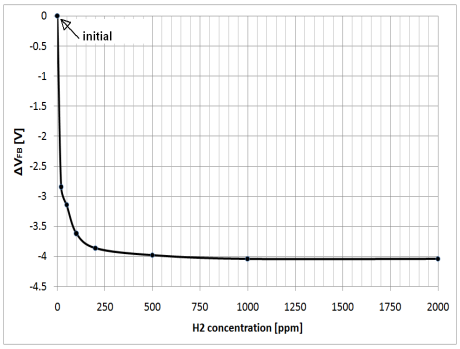

Fig. 10. Flat band voltage shift (ΔV_{FB}) as a function of H_2 concentration (ppm).

The flat band voltage has an important decrease when H_2 concentration increases and reaches a -4 V shift over 500 ppm H_2 concentration. The shift in flat band potential saturates at higher concentrations. All the changes in the voltage take place below 200 ppm.

The reduction of flat band voltage is determined by H_2 adsorption and chemical reactions near the metal-oxide interface [28]. Another mode to use Pd (100nm)/ SiO_2(50nm)/ SiC nanostructure as a gas sensor is to hold the device at a constant capacitance during the time when H_2 gas concentration is changed. In this case the bias voltage of the metal thin film gate required to maintain the constant capacitance is the sensor signal.

Fig. 11 shows the response of a Pd/SiO_2/SiC micro-sensor at different concentrations of H_2, analyzed at fixed measurement temperatures (25°C, 150°C, 200°C).

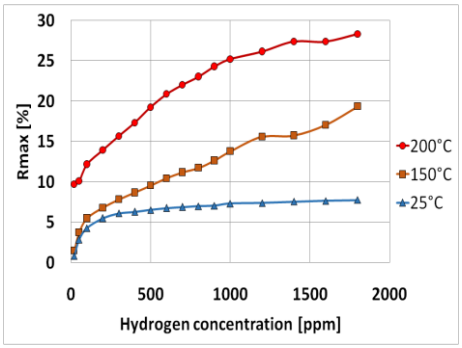

Fig. 11. Variation of maximum response at different concentrations of H_2 (0-2000 ppm), analyzed at fixed measurement temperatures.

Bias voltage at each measurement temperature was: V=5.3 V for 25°C; V=5.8 V for 150°C and V=6 V at 200°C. The tendency of unsaturation of the sensor at higher concentration for high temperatures (over 150°C), is due to the action of hydrogen that is partially eliminated at the metal/oxide interface with the growth of temperature. In conclusion, the increased temperature has an important role in the increased rate of hydrogen desorption.

5. Conclusions

Palladium/silicon oxide/4H-SiC nanostructures with applicability for sensitive detection of hydrogen were studied. The use of SiC wafers for hydrogen sensors is justified by the remarkable properties of SiC semiconductors comparative with silicon semiconductor technology for detection at high temperature and in corrosive environments [29].

The electrical performance of Pd(100nm)/SiO_2(50nm)/SiC nanostructures was analyzed at concentrations ranging from 0 ppm to 2000 ppm H_2. The shift in the C-V curve on the voltage axis is proportional with the adsorption of hydrogen atoms by the metal and oxide layer and the exchange of positive charges between oxide layer and metal-oxide interface.

Operating temperatures up to 150^{o}C show the best detection results. Electrical performance is correlated with the quality of silicon oxide thin film and the palladium thin film, which shows smooth and porous surface, with medium grain size of 20-30 nm.

The sensitivity of Pd/SiO_2/SiC nanostructure as sensor is very good for lower concentration of hydrogen (under 200 ppm H_2).

Acknowledgements

Authors are grateful for funding support from the Romanian Space Agency, project STAR number 190/2017.

References

[1] N. I. Sax, Dangerous Properties of Industrial Materials, in Van Nostrand Reinhold, 4th ed., New York, USA, p. 21, (1975).
[2] G. W. Hunter, NASA Technical Memorandum **105878**, 21 (1982).
[3] T. Hubert, L. Boon-Brett, V. Palmisano, M. A. Bader, International Journal of Hydrogen Energy **39**, 20474 (2014).
[4] P. G. Neudeck, R. S. Okojie, L. Y. Chen, Proceedings of the IEEE **90**, 1065 (2002).
[5] N. G. Wright, A. B. Horsfall, K. Vassilevski, Materials Today **11,** 16 (2008).
[6] M. G. Fontana, Corrosion Engineering, ed. McGraw-Hill, New York, p. 37, (1986).
[7] J. Kittel, V. Smanio, M. Fregonese, L. Garnier, X. Lefebvre, Corrosion Science **52**, 1386 (2010).
[8] G. W. Hunter, P. G. Neudeck , L-.Y. Chen, D. B. Makel, C. C. Liu, Q. H. Wu, NASA Technical Memorandum **208817**, 10 (1998).
[9] A. L. Spetz, A. Baranzahi, P. Tobias, I. Lundstrom, Physica Status Solidi **A 162**, 493 (1997).
[10] I. Lundström, S. Shivaraman, C. Svensson, L. Lundkvist, Applied Physics Letters **26**, 55 1975).
[11] P. F. Ruths, S. Ashok, S. J. Fonash, J. M. Ruths, IEEE Transactions on Electronic Devices **28**, 1003 81).
[12] R. Ghosh, R. Loloee, Proc. IEEE Sensors **12,** 612 (2007).
[13] W. J. Choyke, G. Pensl, MRS Bulletin **3**, 25 (1997).
[14] A. L. Spetz, S. Savage, Silicon Carbide Recent Major Advances, Eds. Springer, Berlin, Germany, p. 870, (2004).
[15] C. Liu, Z. Chen, International Journal of Hydrogen Energy **35**, 12561 (2010).
[16] H. Watanabe, Y. Kokubun, Chemical Sensors **17**, 50 (2001).
[17] F. C. Lin, Y.Takao, V. Shimizu, M. Egashira, Sensors and Actuators **B 24-25**, 843 (1995).
[18] S. Nakagomi, K. Okuda, Y. Kokubun, Sensors and Actuators **B 96**, 364 (2003).
[19] C. Hu, MOS Capacitor" https://people.eecs.berkely.edu/~hu/Chenming-Hu_ch5, (2009).
[20] R. N. Ghosh, P. Tobias, IEEE Trans. Electronic Devices **46**, 561 (1999).
[21] I. Lundström, M. Armgarth, L.-G. Petersson, Solid State and Materials Sciences **15**, 201 (1989).
[22] A. Spetz, A. Arbab, I. Lundström, Sensors and Actuators **B 15**, 19 (1993).
[23] R. N. Ghosh, P. Tobias, G. Ejakov Sally, B. Golding, Proc. of IEEE Sensors **2**, 1120 (2002).
[24] P. Tobias, B. Golding, R. N. Ghosh, IEEE Sensors Journal **2**, 543, (2003).
[25] A. Trinchi, S. Kandasamy, W. Wlodarski, Sensors and Actuators B **133**, 705 (2008).
[26] L. G. Ekedahl, M. Eriksson, I. Lundström, Acc. Chem. Res. **31**, 249 (1995).
[27] T. Hübert, L. Boon-Brett, G. Black, U. Banach, Sensors and Actuators B **157**, 329 (2011).
[28] G. W. Hunter, P. G. Neudeck, M. Gray, D. Androjna, L. Y. Chen, R. W. Hoffman Jr.,

C. C. Liu, Q. H. Wu, Materials Science Forum **338–342**, 1439 (2000).
[29] M. S. Shur, S. Rumyantsev, M. Levinshtein, SiC Materials and Devices vol. 2, Eds. World Scientific Publishing Co. New York, p. 75, (2007).